

## Electrochemical Performance of Nitrogen-Enriched Carbons in Aqueous and Non-Aqueous Supercapacitors

Denisa Hulicova,\* Masaya Kodama, and Hiroaki Hatori

Energy Storage Materials Group, Energy Technology Research Institute, National Institute of Advanced Industrial Science and Technology, 16-1 Onogawa, Tsukuba, Ibaraki 305-8569, Japan

Received January 20, 2006. Revised Manuscript Received February 20, 2006

Carbon materials with significant nitrogen contents were investigated as the electrode materials of supercapacitors. The preparation procedure involved the polymerization of melamine in the interlayer space of template fluorine mica and carbonization at 750, 850, and 1000 °C. Some samples were also stabilized prior to carbonization. We have shown previously that these carbons possess very interesting capacitive behavior in an acidic medium despite small surface areas. High capacitance values in H<sub>2</sub>SO<sub>4</sub> were attributed to the pseudocapacitive interactions between the protons and nitrogen atoms. This paper further discusses the results obtained in a base and an aprotic electrolyte, KOH and TEABF<sub>4</sub>/PC, respectively. Electrochemical properties were evaluated with cycling voltammetry, a galvanostatic charge/discharge technique, and electrochemical impedance spectroscopy. High capacitance values were obtained in proton-free KOH, and the presence of pseudocapacitive interactions between the ions of the electrolyte and the nitrogen atoms of the carbon matrix is proposed. Compared to those in sulfuric acid, greater capacitances of nonstabilized samples were obtained in KOH, i.e., for the sample carbonized at 1000 °C, the capacitance was 84.61 F/g in KOH vs 47.92 F/g in H<sub>2</sub>SO<sub>4</sub>. On the other hand, less porous but more nitrogen-rich stabilized samples gave better performances in H<sub>2</sub>SO<sub>4</sub>, i.e., 62.24 F/g in H<sub>2</sub>SO<sub>4</sub> compared to 49.86 F/g in KOH for the sample stabilized and carbonized at 1000 °C. The sample heat-treated at 750 °C with a surface area of ca. 400 m<sup>2</sup>/g performs similarly in both electrolytes, i.e., ~200 F/g. Significantly lower gravimetric capacitances were obtained in TEABF<sub>4</sub>/PC from the samples carbonized at 750 °C. On the other hand, the almost nonporous sample subjected to stabilization prior to carbonization at 1000 °C gave a capacitance of ~20 F/g. Hence, we suggest that the faradaic interactions between the carbon electrode material and the electrolyte, although much less significant than those in H<sub>2</sub>SO<sub>4</sub> and KOH, play an important role in the nonaqueous electrolyte as well. Narrow micropores were detected by CO<sub>2</sub> adsorption/desorption, and their importance to the interpretation of capacitive behavior is also discussed.

Several reports have been published on the improved capacitive behavior of supercapacitors, electrodes of which were made from carbon materials enriched with nitrogen or oxygen surface functional groups.<sup>1–5</sup> These electrochemically active centers contribute to the overall capacitance, with pseudocapacitance that generally originates from the faradaic interactions between the ions of electrolytes and the carbon electrode surface. The oxygen surface groups, formed in most of the activated carbons during the activation process, have an acidic character, thus introducing electron-acceptor properties into the carbon surface. On the other hand, nitrogen functionalities have generally basic characters, inducing electron-donor properties.<sup>6</sup>

The origin of pseudocapacitance in nitrogen-enriched carbons is yet to be clarified. However, a reasonable assumption is that the nitrogen species located at the periphery of graphene sheets, i.e., pyridinic, pyridonic, and oxidized nitrogen, interact with the ions of electrolytes and therefore are the active species. It should be pointed out that these pseudocapacitive interactions are not purely faradaic in terms of oxidation/reduction reactions, similar to RuOx pseudocapacitors.<sup>7,8</sup> Their advantage is the improvement of electrode wettability because of the increased number of hydrophilic polar sites. In addition, the pseudocapacitance is not a rate-limiting factor, i.e., it is a fast process and therefore these capacitors can be loaded with high-current densities without any significant capacitance loss or increased ohmic drops.<sup>2</sup>

Recently, Lota et al. reported on the capacitors, electrodes of which were prepared by pyrolysis of nitrogen-containing polymers blended with coal tar pitch and subsequent activation.<sup>2</sup> This technique allowed them to prepare carbon material

\* To whom correspondence should be addressed. Tel: 81-29-861-8430. Fax: 81-29-861-8440. E-mail: denisa-hulicova@aist.go.jp.

- (1) Hsieh, C.; Teng, H. *Carbon* **2002**, *40*, 667.
- (2) Lota, G.; Grzyb, B.; Machnikowska, H.; Machnikowski, J.; Frackowiak, E. *Chem. Phys. Lett.* **2005**, *4040*, 53.
- (3) Jurewicz, K.; Babel, K.; Ziolkowski, A.; Wachowska, H.; Kozlowski, M. *Fuel Process. Technol.* **2002**, *77–78*, 191.
- (4) Jurewicz, K.; Babel, K.; Ziolkowski, A.; Wachowska, H. *J. Phys. Chem. Solids* **2004**, *65*, 269.
- (5) Jurewicz, K.; Babel, K.; Ziolkowski, A.; Wachowska, H. *Electrochim. Acta* **2003**, *48*, 1491.
- (6) Vagner, C.; Finqueneisel, G.; Jimmy, T.; Burg, P.; Grzyb, B.; Machnikowski, J.; Weber, J. V. *Carbon* **2003**, *41*, 2847.

- (7) Sarangapani, B.; Tilak, V.; Chen, C. P. *J. Electrochem. Soc.* **1996**, *143*, 3791.
- (8) Ramani, M.; Haran, B. S.; White, R. E.; Popov, B. N. *J. Electrochem. Soc.* **2001**, *148*, A374.

with ca. 7 wt % nitrogen. They found good correlation between the specific capacitance and the nitrogen content for samples with similar microtextural characteristics. The pseudocapacitance was proposed as the reactions of the oxidation/reduction of pyridinic rings, but no redox peaks were observed in cyclic voltammograms. Jurewicz et al. also observed improved capacitive behavior of various carbon materials subjected to the ammoxidation process, i.e., a treatment of nitrogen-free carbons with an ammonia/air mixture in which the nitrogen groups were introduced mainly to the surface of carbon at a concentration of about 2 wt %.<sup>3–5</sup> The extent of nitrogen influence on the capacitive behavior depended on the thermal treatment stage at which the ammoxidation process was introduced, i.e., before or after activation.

Another concept was introduced by Shiraishi et al.<sup>9</sup> They prepared nitrogenous carbon by defluorination of perfluoro organics, such as perfluoropyridine, cyanuric fluoride, etc., with alkaline metals and investigated the capacitive performance of EDLC constructed from this electrode material. The micro/mesoporous carbon with large surface areas of 1000 m<sup>2</sup>/g and 0.02–0.15 nitrogen:carbon atomic ratio showed improved capacitance in the nonaqueous electrolyte. The authors suggested that this is the result of the modification of the space charge layer because of the presence of incorporated nitrogen.

The above-mentioned preparation techniques, though innovative and effective, result in carbon material with relatively low nitrogen content. In addition, the activation process is often employed; therefore, the obtained nitrogen-enriched activated carbons possess a large double-layer capacitance that makes investigation of the pseudocapacitive contribution of nitrogen quite difficult.

Template nitrogen-enriched carbons initially prepared and tested in supercapacitors by our group differ from the nitrogenous carbons described above in a few aspects. First, our carbons are poorly porous and second, the nitrogen contents are significantly higher. Low porosity is the consequence of the original template structure and is also due to the activation process being employed in order to keep the nitrogen content as high as possible. High nitrogen contents are due to careful selection of nitrogen-containing carbon precursors. Expandable fluorine mica (EFM) and various nitrogen-containing organic precursors are used as the template and carbon source, respectively. EFM can be characterized as a tetrahedral and octahedral crystalline network with a two-dimensional spread.<sup>10</sup> The carbon liquid precursors are introduced between the lamellae thanks to their intrinsic dilatibility, and a replica carbon is obtained after carbonization and mica removal. Because of the two-dimensional template structure, the resultant carbon cannot possess a large surface like the template carbon prepared by use of MCM48 or SBA15, which are well-known silica templates for the preparation of ordered, highly porous template carbon.<sup>11–13</sup>

(9) Shiraishi, S.; Kibe, M.; Oya, A. *International Conference on Carbon, Carbon 2004*, July 11–16, 2004; Abstract 23.1.

(10) Tateyama, H.; Nishimura, S.; Tsunematu, K.; Jinnai, K.; Adachi, Y.; Kimura, M. *Clays Clay Miner.* **2002**, *23*, 180.

(11) Yoon, S. B.; Kim, J. Y.; Yu, J. S. *Chem. Commun.* **2001**, *06*, 559.

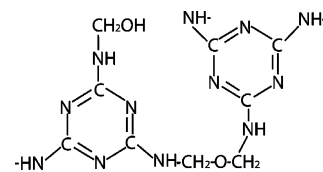


Figure 1. Structure of melamine resins.

Initially, using EFM as the template and quinoline as the carbon precursor, we prepared a very unique carbon.<sup>14</sup> The structure consisted of thin amorphous carbon film laced with an ordered carbon rim. Apart from the structural uniqueness, the electrochemical properties were also very interesting. Despite a small surface area (less than 90 m<sup>2</sup>/g), the gravimetric capacitance of a supercapacitor manufactured from this material was ca. 100 F/g. When pyridine, which contained more nitrogen atoms in its structure and therefore had more nitrogen atoms in the carbon material after heat treatment, was used as carbon precursor, the capacitive behavior increased to ca. 150 F/g. These results suggested that even poorly porous carbon that is rich in nitrogen can serve as promising electrode material in supercapacitors. The highest nitrogen content after heat treatment at 800 °C was still only ca. 10 wt %. Therefore, we were eager to employ a different carbon precursor that would allow us to prepare carbon material with abundant nitrogen residue. Through careful selection, we prepared an EFM template nitrogen-enriched carbon from melamine resins.<sup>15</sup> Melamine resin is a polymer that contains 45 wt % nitrogen in its polymeric state and is therefore a very suitable precursor (Figure 1). Nitrogen volatilities are released gradually with an applied temperature up to 850 °C and released rapidly with further temperature increases. However, almost 8 wt % nitrogen remains present in the carbon matrix after heat treatment at 1000 °C. Furthermore, it is a cheap and commercially available polymer often used in various applications.<sup>16,17</sup>

An important step in the preparation of melamine-based carbon is the stabilization process conducted in an oxidative atmosphere at 200–250 °C. We found that this treatment not only increased the carbon yield but also preserved the nitrogen atoms in the carbon matrix during the carbonization process. Therefore, the stabilized samples contain more nitrogen than the nonstabilized ones when they are carbonized at the same temperatures (Figure 2a).

In our previous report, we evaluated the electrochemical behavior of the EFM template melamine-based carbons in aqueous electrolytes of sulfuric acid and sodium chloride in a three-electrode-cell arrangement. The extra high values of the gravimetric capacitance, ca. 200 F/g, and especially the capacitance per surface area, 1.5 F/m<sup>2</sup> in acidic medium, were elucidated, whereas those values in a neutral medium were

(12) Ryoo, R.; Joo, S. H.; Jun, S. *J. Phys. Chem. B* **1999**, *103*, 7743.

(13) Vinu, A.; Murugesan, V.; Hartmann, M. *J. Phys. Chem. B* **2004**, *108*, 7323.

(14) Kodama, M.; Yamashita, J.; Soneda, Y.; Hatori, H.; Nishimura, S.; Kamegawa, K. *Mater. Sci. Eng., B* **2004**, *108*, 156.

(15) Hulicova, D.; Yamashita, J.; Soneda, Y.; Hatori, H.; Kodama, M. *Chem. Mater.* **2005**, *17* (5), 1241.

(16) Derylo-Marczewska, A.; Goworek, J.; Kusak, R.; Zgrajka, W. *Appl. Surf. Sci.* **2002**, *195*, 117.

(17) Biggs, S.; Lukey, C. A.; Spinks, G. M.; Yau, S.-T. *Prog. Org. Coat.* **2001**, *42* (1–2), 49.

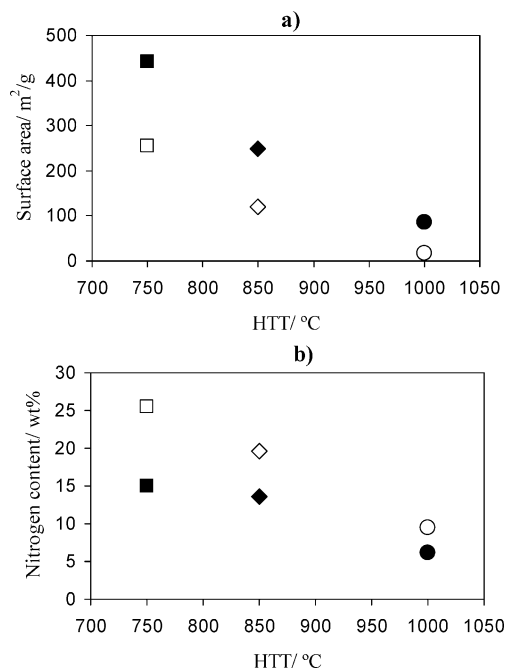


**Figure 2.** (a) Relation between the surface area and heat-treatment temperature HTT; (b) relation between the nitrogen content evaluated by the combustion method and HTT. Solid and open symbols represent nonstabilized and stabilized samples, respectively.

more or less in the range of double-layer capacitance, i.e., 74.29 F/g and 0.17 F/m<sup>2</sup>, respectively, for the same sample. We also found that the stabilized samples possessed better capacitive behavior in H<sub>2</sub>SO<sub>4</sub> despite smaller surface areas. Importantly, the nitrogen contents of these samples were much higher compared with their nonstabilized counterparts; from the XPS study, we understood that they contained more pyridinic nitrogen located at the periphery of the graphene sheets, which is in agreement with the studies of Pinero et al.<sup>18</sup> Similarly, they noticed an enrichment of nitrogen species in the surface of melamine-based carbons after stabilization. This fact is very beneficial for electrochemical applications, because the surface of the electrode material is the most accessible to the electrolyte and therefore is the most electrochemically active.

According to that, we logically assigned the improved capacitance behavior of stabilized samples in H<sub>2</sub>SO<sub>4</sub> to the extent of nitrogen species at the edges of graphene sheets.

In this report, we further evaluated the electrochemical properties of these carbons in a base electrolyte of potassium hydroxide (KOH) and a nonaqueous or so-called aprotic electrolyte of tetraethylammonium tetrafluoroborate in propylene carbonate (TEABF<sub>4</sub>/PC) using three-electrode-cell layouts. Cyclic voltammetry, galvanostatic charge/discharge techniques, and electrochemical impedance spectroscopy were used for this purpose. Our previous communication discusses the XPS, FE-SEM, nitrogen adsorption/desorption, and elemental analysis of melamine-based carbons. Here, to characterize the porous structure further, we also performed CO<sub>2</sub> adsorption/desorption measurements. In addition, the resistance of each pellet to electrochemical measurements in the dry state was measured by a four-probe technique.

## Experimental Section

### 1. Preparation and Characterization of Carbon Samples.

Details of the preparation procedure of the EFM template melamine-based carbons were presented elsewhere.<sup>15</sup> In short, melamine was mixed with formaldehyde and EFM and subjected to polymerization at 80 °C for 30 min. The samples were then carbonized at 750, 850, and 1000 °C, and pure nitrogen-enriched carbon specimens were obtained after mica removal with HCl/HF treatment. These samples are denoted as Me750, Me850, and Me1000 hereafter. Another group of samples was obtained when the sample after polymerization was subjected to stabilization at 250 °C in air prior to carbonization. The following carbonization proceeded at the same temperatures, and these samples are labeled Me750s, Me850s, and Me1000s.

CO<sub>2</sub> adsorption isotherms at 298 K were recorded using Belsorp18, a Bel Japan Inc. instrument. The microporosity volumes were obtained from CO<sub>2</sub> adsorption data by applying the Dubinin–Radushkevich (DR) equation and considering the density of CO<sub>2</sub> to be 1.56 g/cm<sup>3</sup>.

**2. Electrochemical Measurements.** Pellets for the electrochemical measurements were prepared by mixing the carbonized sample with carbon black (Mitsubishi Chemicals Inc.) and a poly(tetrafluoroethylene) binder (PTFE, Mitsui Dupont Fluorochemicals, 7A-J, Inc.). The sample:CB:PTFE ratio was kept at 80:10:10 wt %. The ammonium hydrocarbonate added in a 1:1 sample:NH<sub>4</sub>-HCO<sub>3</sub> ratio by weight was expected to form small pores in a pellet during its decomposition in the drying process (110 °C in a vacuum); these pores should promote electrolyte diffusion. The sample was pressed at 40 MPa for 15 min and afterward rolled to the thickness of ca. 100 μm. The final pellet diameter was set at 1 cm, and the mass was ca. 8 mg. Cyclic voltammetry (CV), galvanostatic charge/discharge cycling (GC), and electrochemical impedance spectroscopy (EIS) were employed in the evaluation of electrochemical behavior of each sample. The electrochemical performances of samples were evaluated in two electrolytes, i.e., 6 M potassium hydroxide (KOH) and 1 M tetraethylammonium tetrafluoroborate in propylene carbonate (TEABF<sub>4</sub>/PC). All experiments were carried out at room temperature in a standard three-compartment cell. Platinum foil and platinum mesh were used as the counter electrode and current collector, respectively, for both electrolytes. Hg/HgO and Ag/AgCl were chosen as the reference electrodes for KOH and TEABF<sub>4</sub>/PC, respectively.

GC measurements with a current loading of 20 mA/g were conducted on a multichannel VMP potentiostat/galvanostat (multichannel potentiostats/galvanostat VMP-80, Princeton Applied Research). A potential range from −1 to 0 V vs Hg/HgO was applied in KOH. In the case of TEABF<sub>4</sub>/PC, galvanostatic charge/discharge curves were recorded in a potential range between −1.5 and 0.5 V vs Ag/AgCl.

The specific gravimetric capacitances were calculated from the discharge process of the 10th cycle on the basis of eq 1

$$C_g = I\Delta t/\Delta V \quad (1)$$

where  $C_g$  is the specific gravimetric capacitance (F/g),  $I$  is the current loaded,  $\Delta t$  is the discharge time (s), and  $\Delta V$  is the potential change during the discharge process.

Specific capacitances per surface area  $C_s$  (F/m<sup>2</sup>) were also calculated using eq 2

$$C_s = C_g/SA \quad (2)$$

where SA is a total surface area (m<sup>2</sup>/g) calculated from  $\alpha_s$  plots.

(18) Raymundo-Pinero, E.; Cazorla-Amoros, D.; Linares-Solano, A.; Find, J.; Wild, U.; Schlogl, R. *Carbon* **2002**, *40*, 597.



**Table 1. Micropore Volumes Evaluated from CO<sub>2</sub> and N<sub>2</sub> Adsorption/Desorption Techniques**

sample	V <sub>micro</sub> CO <sub>2</sub> (cm <sup>3</sup> /g)	V <sub>micro</sub> N <sub>2</sub> (cm <sup>3</sup> /g)
Me750	0.29	0.13
Me850	0.08	0.06
Me1000	0.06	0.01
Me750s	0.12	0.07
Me850s	0.04	0.02
Me1000s	0.04	0.01

CV measurements in both electrolytes were performed using the same cell layouts and potential ranges, with a potential scan rate of 1 mV/s.

Impedance measurements were conducted in KOH over a frequency range from 100 kHz to 10 mHz, and a polarization potential of -0.4 V was applied.

The resistance of dry pellets was measured by a four-probe technique using Loresta-GP MCP-T600 equipment (Mitsubishi Chemical Corp. Ltd.).

### Results and Discussion

The basic characteristics of all samples, such as surface areas and nitrogen contents, have been reported already<sup>15</sup> and are therefore not discussed here in detail. The result summary is shown in Figure 2. Figure 2a represents the relation between the heat-treatment temperature (HTT) and the surface area of each sample. One can see that the surface area decreases with the HTT and that the stabilized samples are less porous than the nonstabilized ones. In contrast, the nitrogen contents, evaluated by the CHN combustion method, are higher in stabilized samples (Figure 2b). In conclusion, the stabilized samples were found to be less porous but richer in nitrogen residues compared to their nonstabilized counterparts.

Table 1 displays the micropore volumes estimated from DR plots of CO<sub>2</sub> adsorption at 298 K. They are compared with the micropore volumes obtained from N<sub>2</sub> adsorption/desorption isotherms at 77 K, presented earlier.<sup>15</sup> It is clear that the values resulting from CO<sub>2</sub> measurements are noticeably higher than those from N<sub>2</sub> adsorption/desorption. Such a discrepancy can be attributed to the presence of ultra micropores that cannot be detected by nitrogen molecules because of their diffusional problems into the narrow micropores of less than 0.7 nm and the density problems of the adsorptive. CO<sub>2</sub> molecules, on the other hand, are adsorbed at higher temperatures and therefore their kinetic energies are larger, which allows them to enter the narrow pores, and the volumes of these micropores can be calculated. Comprehensive studies made especially by the Linares-Solano group demonstrated that in order to well-characterize the microporous structure of less-porous carbons and to avoid the underestimation of microporosity, it is highly recommended to perform both the nitrogen and carbon dioxide adsorption/desorption measurements.<sup>19,20</sup> This fact appears to be relevant for our samples. Therefore, it can be said that all samples contain larger fractions of narrow micropores than estimated initially with the nitrogen adsorption/desorp-

**Table 2. Resistance of Dry Pellets for Electrochemical Measurements Evaluated with a Four-Probe Technique**

sample	R <sub>pellet</sub> press&roll (Ω cm)	R <sub>pellet</sub> press (Ω cm)
Me750	59.99	208.81
Me850	4.02	5.88
Me1000	0.49	0.53
Me750s	90.79	274.83
Me850s	19.09	22.84
Me1000s	0.93	4.42

tion measurements. However, they can still be considered as being poorly porous carbons, and their high values of capacitances obtained in an acidic medium can be attributed to the presence of nitrogen atoms and resultant pseudocapacitance rather than the underestimated double-layer capacitance from the ion electrosorption on these narrow micropores.

The resistance values of dry pellets are shown in Table 2. To investigate the effectiveness of rolling process on the electrical conductivity, we also measured the resistances of pellets after pressing and before rolling. The resistance decreases markedly with HTT; for example, the values for Me750 and Me1000 are 59.99 and 0.49 Ω cm, respectively. It is well-known that the structure of carbon becomes more ordered at higher temperatures, which leads to the improved electrical conductivity. Hence, the obtained data are reasonable. It was also found that the stabilized samples were less conductive, as the resistances of Me750s and Me1000s are 90.79 and 0.93 Ω cm, respectively. The reason for this may be the presence of more nitrogen species on the surface of these samples than on the nonstabilized ones. From the data of pressed-only pellets, we can conclude that the rolling process improved the electrical conductivity of all samples. Particularly, the intraparticle resistance is expected to be lowered, which is a very important factor in capacitor performance. Another benefit of the rolling procedure was the possibility of preparing very thin pellets, ca. 70–100 μm. By simple pressing, the average thickness of pellets was ca. 400 μm.

To further demonstrate the interesting electrochemical behavior of melamine-based template carbon, we present results on the capacitive performance in an aqueous media of KOH.

Nyquist plots, which represent the frequency responses of the samples and are commonly used to present and analyze EIS data, reflect the conductive properties of carbons (Figure 3). Generally, the high-frequency region represents the sum of the internal resistance of the carbon material, electrolyte resistance, and contact resistance between the working electrode and the current collector. Although it is almost impossible to prepare identical cell layouts, we used the same technique in assembling each cell. In addition, the same electrolyte was used, and it may therefore be considered that the high-frequency region more or less reflects the conductive properties of the carbon electrode material.

From the intensity of semicircle, it is clear that the intrinsic resistance of carbon changes with HTT. Very large internal resistance is observed in Me750 and Me750s. It becomes smaller with increased HTT for both the nonstabilized and stabilized samples, suggesting a lowering of the carbon intrinsic resistance. Because the semicircle is also associated

(19) Gariddo, J.; Linares-Solano, A.; Martin-Martinez, J. M.; Molina-Sabio, M.; Rodriguez-Reinoso, F.; Torregrosa, R. *Langmuir* **1987**, *3*, 76.

(20) Lozano-Castello, D.; Cazorla-Amoros, D.; Linares-Solano, A. *Carbon* **2004**, *42*, 1233.

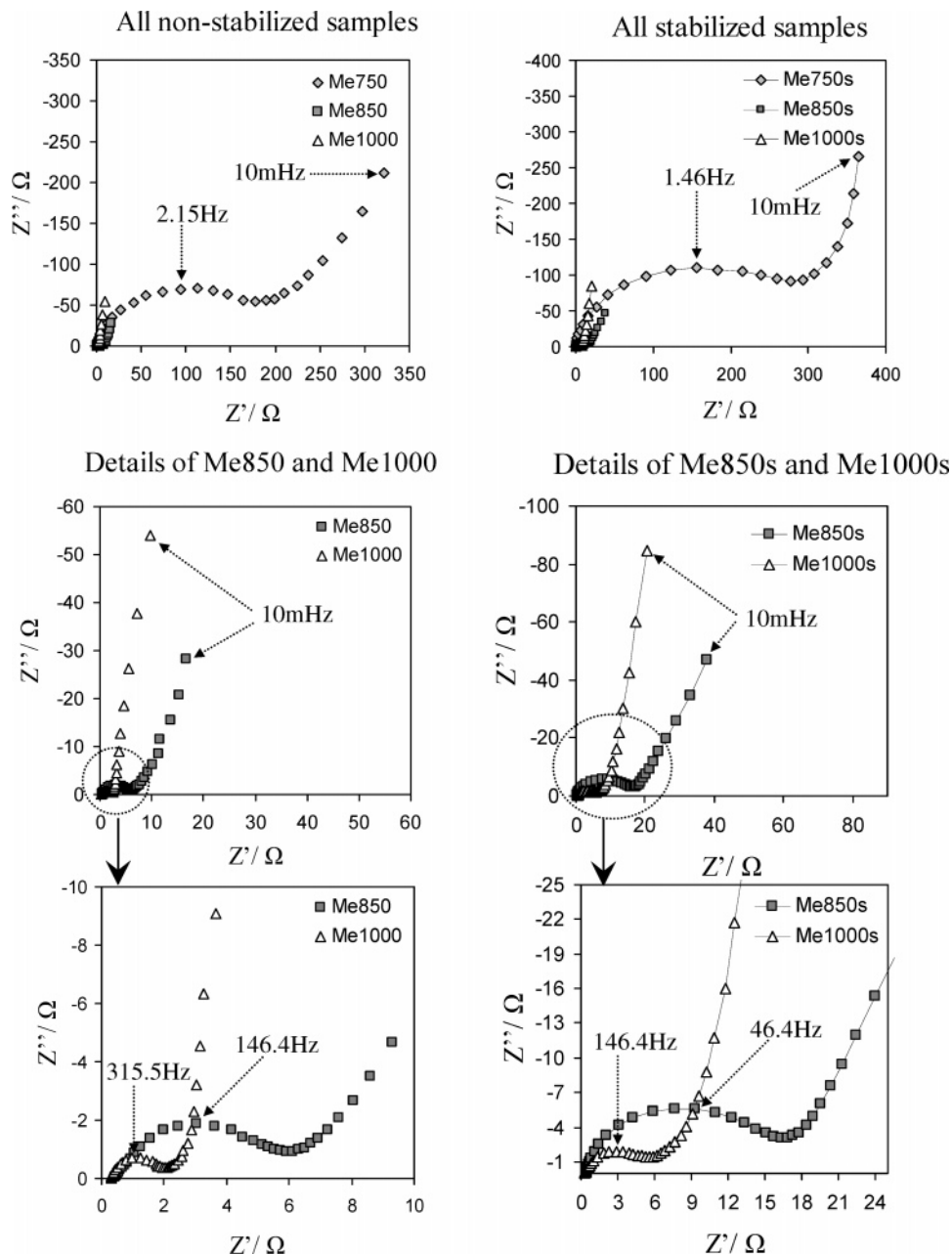


**Figure 3.** Nyquist plots of nonstabilized and stabilized samples recorded in 6 M KOH, three-electrode cell, applied voltage  $-0.4$  V vs Hg/HgO, frequency range of 100 kHz to 10 mHz. Detailed plots of Me850, Me1000, Me850s, and Me1000s are also shown separately.

with the pseudocapacitive interactions,<sup>21</sup> we can conclude that the stabilized samples with higher nitrogen contents and larger loops show the presence of faradaic pseudocapacitive interaction to a greater extent than the nonstabilized ones.

The imaginary part of the impedance spectra at low frequencies represents the capacitive behavior of the electrode and approaches a  $90^\circ$  vertical line in an ideal capacitor.<sup>22</sup> Obviously, the supercapacitors manufactured from melamine-based carbons are not ideal and, therefore, the low-frequency parts of Nyquist plots incline. The differences between the ideal and experimental capacitors were also observed in pseudocapacitance-free samples. Song et al.<sup>23</sup> described the

mathematical model for a series of activated carbons with no faradaic interactions in which the pore size distribution was responsible for this phenomenon. In other words, in the carbon electrode materials with uniform pore size distribution, the in-a-pore dispersion claims responsibility for the deviation from the ideal response at high-frequency region, but as penetrability increases with lowering frequency, the impedance approaches  $90^\circ$ . However, the samples with the wide pore distribution differ from the ideal performance in the low-frequency region. The reason is that the penetration of the ac signal is different at the same frequency because of the pore size variations, i.e., the large pores are easily accessible by the electrolyte, whereas the narrow micropores are not. The resulting impedance spectrum is characterized

(21) Gamby, J.; Taberna, P. L.; Simon, P.; Fauvarque, J. F.; Chesneau, M. *J. Power Sources* **2001**, *101*, 109.

(22) Conway, B. E. *Electrochemical Supercapacitors: Scientific Fundamentals and Technological Applications*; Kluwer-Plenum Press: New York, 1999.

(23) Song, H. K.; Hwang, H. Y.; Lee, K. H.; Dao, L. H. *Electrochim. Acta* **2000**, *45*, 2241.

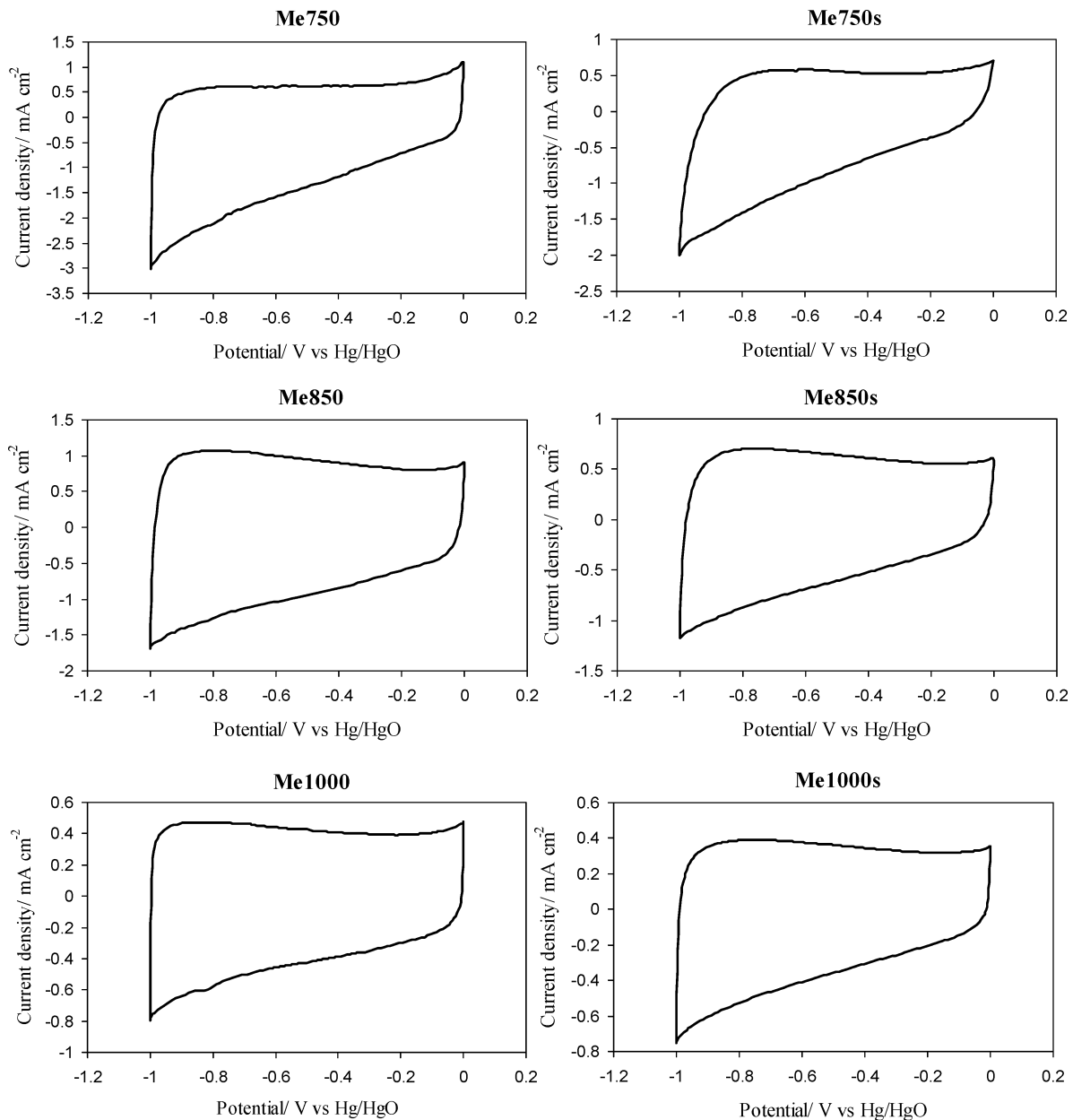


**Figure 4.** Cyclic voltammograms of all samples recorded in 6 M KOH, potential range  $-1$  to  $0$  V vs Hg/HgO, sweep rate =  $1$  mV/s, three-electrode cell. The thickness and mass of the electrode were ca.  $100 \mu\text{m}$  and  $8$  mg, respectively.

by the inclined Nyquist curve. Considering the porous nature of the presented samples, all consist of a mixture of micro-, meso-, and macropores. Hence, the pore size distribution role seems to be accurate in our case. Additionally, one can easily notice the propensity of samples carbonized at  $1000^\circ\text{C}$  to respond toward  $90^\circ$  in the low-frequency region. This may be due to the partial elimination of the effect of pore size distribution because these samples are poorly porous.

The cycling voltammograms of all samples in KOH recorded in the potential range between  $-1$  and  $0$  V vs Hg/HgO are shown in Figure 4. Interestingly, the nonrectangular shapes, similar to those in the cyclic voltammograms of same samples recorded in sulfuric acid, were observed. Clearly enhanced capacitance can be observed in the negative potentials of adsorption/desorption of positively charged ions. The same phenomenon was observed in  $\text{H}_2\text{SO}_4$ , for which protons were preferably adsorbed on the carbon electrode surface.<sup>15</sup> The capacitances per mass and per surface area

**Table 3. Gravimetric Capacitances ( $C_g$ ) and Capacitances per Surface Area ( $C_{SA}$ ) of All Samples in KOH<sup>a</sup>**

sample	KOH		$\text{H}_2\text{SO}_4^b$	
	$C_g$ (F/g)	$C_{SA}$ (F/m <sup>2</sup> )	$C_g$ (F/g)	$C_{SA}$ (F/m <sup>2</sup> )
Me750	208.15	0.47	204.8	0.46
Me850	174.31	0.70	157.4	0.63
Me1000	84.61	0.98	47.92	0.55
Me750s	126.01	0.49	200.1	0.78
Me850s	119.43	0.59	195.9	1.63
Me1000s	49.86	2.93	62.24	3.66

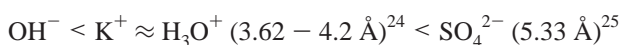
<sup>a</sup> Galvanostatic conditions: current density =  $20$  mA/g, potential range  $-1$  to  $0$  V vs Hg/HgO. For illustration purposes, the capacitances of same samples recorded in  $\text{H}_2\text{SO}_4$  reported earlier are also listed. <sup>b</sup> See ref 15.

of electrode material calculated from galvanostatic charge/discharge measurements are summarized in Table 3. Capacitances of same samples in  $\text{H}_2\text{SO}_4$  reported earlier are also shown for comparison purposes. Regarding the theory of strong pseudocapacitive interactions between the protons and the nitrogen atoms of the carbon electrode in  $\text{H}_2\text{SO}_4$ ,

one would expect capacity loss in a proton-free electrolyte. However, a high capacitance value of 208 F/g for Me750 was obtained in KOH. This is almost the same value as the one obtained in sulfuric acid. Furthermore, Me1000 performed remarkably better in KOH compared to H<sub>2</sub>SO<sub>4</sub>, as the obtained capacitance is 84.61 F/g versus 47.92 F/g. Taking into account the sloped shape of the cathodic branch of the cycling voltammograms, we found that the presence of pseudocapacitive interactions between the positively charged ions, in this case the potassium cations and the nitrogen atoms of carbon, are highly liable. The improved capacitance in KOH was observed for nonstabilized samples, whereas the capacitance loss was measured in stabilized samples.

Apart from the pseudocapacitive contribution of nitrogen atoms, a very important factor, which is the different ion size of KOH and H<sub>2</sub>SO<sub>4</sub>, should be considered when interpreting the capacitive performance of nitrogenous carbon. It is well-known that in the aqueous electrolytes, the positively charged ions are presented and thus adsorbed in the hydrated form. Eliad et al. reported the size of potassium ion K<sup>+</sup> to be similar to that of protic ion H<sub>3</sub>O<sup>+</sup>, i.e., within the range 3.62–4.2 Å.<sup>24</sup> Because the size of bare K<sup>+</sup> is 2.66 Å, the dimensional importance of the hydration shell is quite significant. The negatively charged ions, on the other hand, are adsorbed in the bare state in most cases, except for bivalent sulfate SO<sub>4</sub><sup>2-</sup> ions. Endo et al. used the COSMO method to compute the possible structure of hydrated SO<sub>4</sub><sup>2-</sup> and found out that the most likely number of hydrates was 12.16 molecules of water per one SO<sub>4</sub><sup>2-</sup> ion and the calculated size of SO<sub>4</sub><sup>2-</sup>(H<sub>2</sub>O)<sub>12</sub> was estimated to be 5.33 Å.<sup>25</sup> The hydroxide anions OH<sup>-</sup> are adsorbed in the bare state and thus their size is smaller than that of SO<sub>4</sub><sup>2-</sup> and also K<sup>+</sup>.

In conclusion, the dimensional order of ions of aqueous electrolytes used in this experiment is as follows



For all these reasons, very narrow micropores demonstrated by CO<sub>2</sub> adsorption/desorption could accommodate tiny OH<sup>-</sup> in contrast to large SO<sub>4</sub><sup>2-</sup> and therefore the double-layer contribution of OH<sup>-</sup> electroadsorption to the overall capacitance in KOH is more significant than that of SO<sub>4</sub><sup>2-</sup> in H<sub>2</sub>SO<sub>4</sub>.

High capacitances per surface areas in KOH ranging from ca. 0.47 F/m<sup>2</sup> for Me750 to 0.98 F/m<sup>2</sup> for Me1000 also clearly prove the presence of pseudocapacitive contribution to the overall capacitance. Similar to the performance in H<sub>2</sub>SO<sub>4</sub>, large values for stabilized samples (between 0.49 F/m<sup>2</sup> for Me750s and 2.93 F/m<sup>2</sup> for Me1000s) suggest a more-significant pseudocapacitive contribution to the overall capacitance in these samples than in the nonstabilized ones.

On the basis of the fact that positively charged hydrated ions of both electrolytes, i.e., K<sup>+</sup> and H<sub>3</sub>O<sup>+</sup>, have similar

**Table 4. Gravimetric Capacitances (C<sub>g</sub>) and Capacitances per Surface Area (C<sub>SA</sub>) of Samples Heat-Treated at 750 and 1000 °C in 1 M TEABF<sub>4</sub>/PC<sup>a</sup>**

sample	C <sub>g</sub> (F/g)	C <sub>SA</sub> (F/m <sup>2</sup> )
Me750	37.49	0.08
Me1000	30.48	0.35
Me750s	26.23	0.10
Me1000s	20.61	1.21

<sup>a</sup> Galvanostatic conditions: current density = 20 mA/g, potential range -1.5 to 0.5 V vs Ag/AgCl.

sizes, their nonfaradaic electrosorption should theoretically result in similar capacitances at cathodic branches of cyclic voltammograms. Experimentally obtained different values must therefore result in the presence of different faradaic interactions between the ions and the nitrogen atoms. Considering the capacitive performances of all samples in KOH and H<sub>2</sub>SO<sub>4</sub>, some conclusions can be made.

First, the significant presence of pseudocapacitive interactions is clear in H<sub>2</sub>SO<sub>4</sub> as well as in KOH. Second, despite the difficulties of SO<sub>4</sub><sup>2-</sup> ions in penetrating the pores, especially in poorly porous stabilized samples, very high capacitances were obtained. Some samples showed worse capacitive behavior in KOH even though the OH<sup>-</sup> ions are smaller than SO<sub>4</sub><sup>2-</sup> and thus more easily electroadsorbed on the pores. This suggests that the faradaic interactions between H<sub>3</sub>O<sup>+</sup> and the nitrogen functionalities are stronger than those of K<sup>+</sup> and that they determine the overall capacitive performance.

The remaining question is why no faradaic interactions were observed in a neutral medium of NaCl reported earlier.<sup>15</sup> More research has to be done to clarify this, but at this stage, the acidity and/or the basicity of the electrolyte seem to play an important role.

The electrochemical properties of samples heat-treated at 750 and 1000 °C were further investigated in nonaqueous (aprotic) electrolyte TEABF<sub>4</sub>/PC. The use of aprotic electrolytes is in high demand because of their large potential windows (2–2.7 V). Because the energy density is equal to the square of the applied potential, larger energy densities compared to those of the aqueous electrolytes (~1 V) can be obtained from capacitors containing these electrolytes.

Corresponding capacitances calculated from the galvanostatic charge/discharge technique between -1.5 and 0.5 V vs Ag/AgCl are shown in Table 4. Compared to the aqueous electrolytes, significant capacitance loss is observed in samples carbonized at 750 °C, i.e., 37.49 F/g for Me750 and 26.23 F/g for Me750s. These are the samples with the largest surface areas among tested specimens and they provide the maximum gravimetric capacitances in aqueous media. Interestingly, high values of capacitances are obtained from samples carbonized at 1000 °C, i.e., 30.48 F/g for Me1000 and 20.61 F/g for Me1000s. These are even slightly greater than the values obtained from the same samples in a neutral aqueous electrolyte of NaCl (20.85 F/g for Me1000 and 15.74 F/g for Me1000s).<sup>15</sup>

Like the ion hydration effect in aqueous electrolyte, the solvation of ion in nonaqueous electrolyte must be considered. The ionic radii of TEA<sup>+</sup> and BF<sub>4</sub><sup>-</sup> in PC have been reported to be 3.43 and 2.29 Å, respectively and hence the

(24) Eliad, L.; Salitra, G.; Soffer, A.; Aurbach, D. *J. Phys. Chem B* **2001**, *105*, 6880.

(25) Endo, M.; Maeda, T.; Takeda, T.; Kim, Y. J.; Koshiba, K.; Hara, H.; Dresselhaus, M. S. *J. Electrochem. Soc.* **2001**, *148* (8), A910.



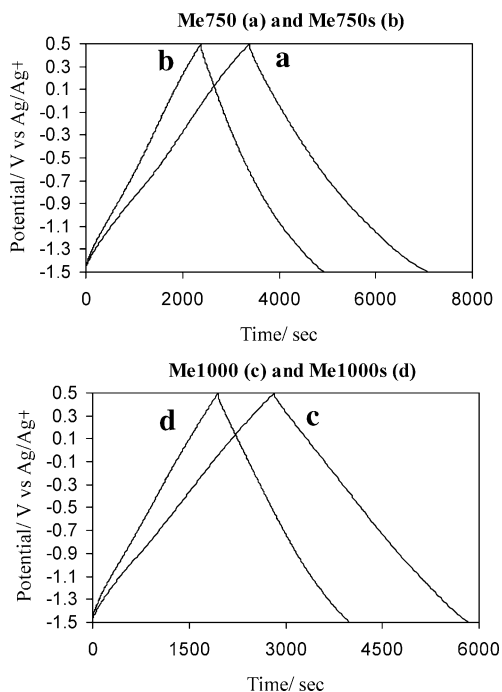
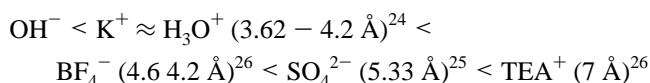


**Figure 5.** Galvanostatic charge/discharge curves of (a) Me750, (b) Me750s, (c) Me1000, and (d) Me1000s. Galvanostatic conditions: 1 M TEABF<sub>4</sub>/PC, current loading = 20 mA/g, potential range -1.5 to 0.5 V vs Ag/AgCl.

effective ion size can be estimated to be around 7 Å for TEA<sup>+</sup> and 4.6 Å for BF<sub>4</sub><sup>-</sup>.<sup>26</sup>

Including the hydrated ions of aqueous electrolytes, the following scale of effective ion size used in this work can be created



Obviously, the ions of nonaqueous electrolytes are larger than the alkali ions, especially the positively charged TEA<sup>+</sup>; therefore, it is very interesting that the less-porous samples serve as more-effective electrode materials in nonaqueous supercapacitors than do the porous samples. From the pore parameters evaluated with the N<sub>2</sub> adsorption/desorption technique at 77 K reported earlier,<sup>15</sup> it is clear that all samples, except for Me1000s, possess enough wide micropores to accommodate the largest TEA<sup>+</sup>. However, the dominant micropore fraction of Me750 seems to be ineffective in sorption of these ions (surface area = 442 m<sup>2</sup>/g, gravimetric capacitance = 37.49 F/g). On the other hand, Me1000s, which has a surface area of only 17 m<sup>2</sup>/g and thus a negligible micropore fraction, provides a capacitance of 20.61 F/g.

Figure 5 shows the galvanostatic charge/discharge characteristics of tested samples. It is interesting that samples carbonized at 750 °C show good electric conductivities as the IR drops are minimal (Figure 5a). As expected, the IR drops of Me1000 and Me1000s are also very small (Figure 5b). In addition, the triangular shapes reflect good capacitive performance.

The cycling voltammograms are displayed in Figure 6. The boxlike shapes suggest the electrosorption of ions on a double layer with no significant faradaic interactions, similar to KOH and/or H<sub>2</sub>SO<sub>4</sub>. However, taking into account the fact that capacitors manufactured from highly porous activated carbons with surface areas of more than 1000 m<sup>2</sup>/g possess gravimetric capacitances of about 80–100 F/g in an aprotic medium, we observed values between ca. 20 and 30 F/g in Me1000s and Me1000. This suggests that even in a nonaqueous electrolyte, some kind of faradaic interactions may occur between the nitrogen species and the ions. These do, however, contribute less to the overall capacitance than the ones present in KOH and H<sub>2</sub>SO<sub>4</sub>.

## Conclusions

The preparation of nitrogen-enriched carbons from melamine resins and their electrochemical performances in H<sub>2</sub>SO<sub>4</sub> and NaCl were reported in our previous communication.<sup>15</sup> Here, we further described the evaluation of these electrochemically interesting materials in KOH and TEABF<sub>4</sub>/PC.

Using cyclic voltammetry and a galvanostatic charge/discharge technique, we measured higher capacitances of nonstabilized samples in KOH compared to those in H<sub>2</sub>SO<sub>4</sub>, i.e., for Me1000, it was 84.61 F/g in KOH vs 47.92 F/g in H<sub>2</sub>SO<sub>4</sub>. On the other hand, less-porous but more nitrogen-rich stabilized samples gave better performances in H<sub>2</sub>SO<sub>4</sub>, i.e., 62.24 F/g in H<sub>2</sub>SO<sub>4</sub> compared to 49.86 F/g in KOH for Me1000s. We concluded that it is essential to consider the effective size of ions when comparing the capacitances in both electrolytes. The positively charged hydrated K<sup>+</sup> and H<sub>3</sub>O<sup>+</sup> are similar in size, whereas the negatively charged ions differ significantly. Sulfate ion SO<sub>4</sub><sup>2-</sup> is electroadsorbed in a hydrated form, in contrast to the hydroxide ion OH<sup>-</sup> of KOH, which is adsorbed in a bare state. Therefore, the double-layer contribution of OH<sup>-</sup> electrosorption on pores is greater than that of SO<sub>4</sub><sup>2-</sup>. This becomes more significant in nonstabilized samples, which are more porous than their stabilized counterparts, and this phenomenon is thought to be responsible for their higher capacitances in KOH. CO<sub>2</sub> adsorption/desorption measurements also supported this assumption when the presence of ultramicropores, which are able to accommodate small OH<sup>-</sup> ions, was confirmed. We also concluded that despite the improved electrosorption of OH<sup>-</sup>, high overall capacitances could not result from only the nonfaradaic electrosorption of ions on the pores. The enhanced capacitances in the cathodic branches of cyclic voltammograms clearly showed the presence of the faradaic interaction between the K<sup>+</sup> and nitrogen atoms. In addition, obtained capacitances per surface areas ranging from 0.45 to 2.93 F/m<sup>2</sup> support this conclusion, as they are much higher than the typical values for activated carbons (~0.2 F/m<sup>2</sup>).

Electrochemical impedance spectroscopy revealed that the intrinsic resistance of the carbon electrode material decreases with heat-treatment temperature. The inclined character of Nyquist plots in the low-frequency region was concluded to be the consequence of pore size distribution.

The capacitive performances in nonaqueous electrolytes were also investigated. In general, remarkably lower capacitances were measured compared to those in aqueous elec-

(26) Ue, M. *J. Electrochem. Soc.* **2004**, *141*, 3336.

(27) Arulepp, M.; Permann, L.; Leis, J.; Perkson, A.; Rumma, K.; Janes, A.; Lust, E. *J. Power Sources* **2004**, *133* (2), 320.



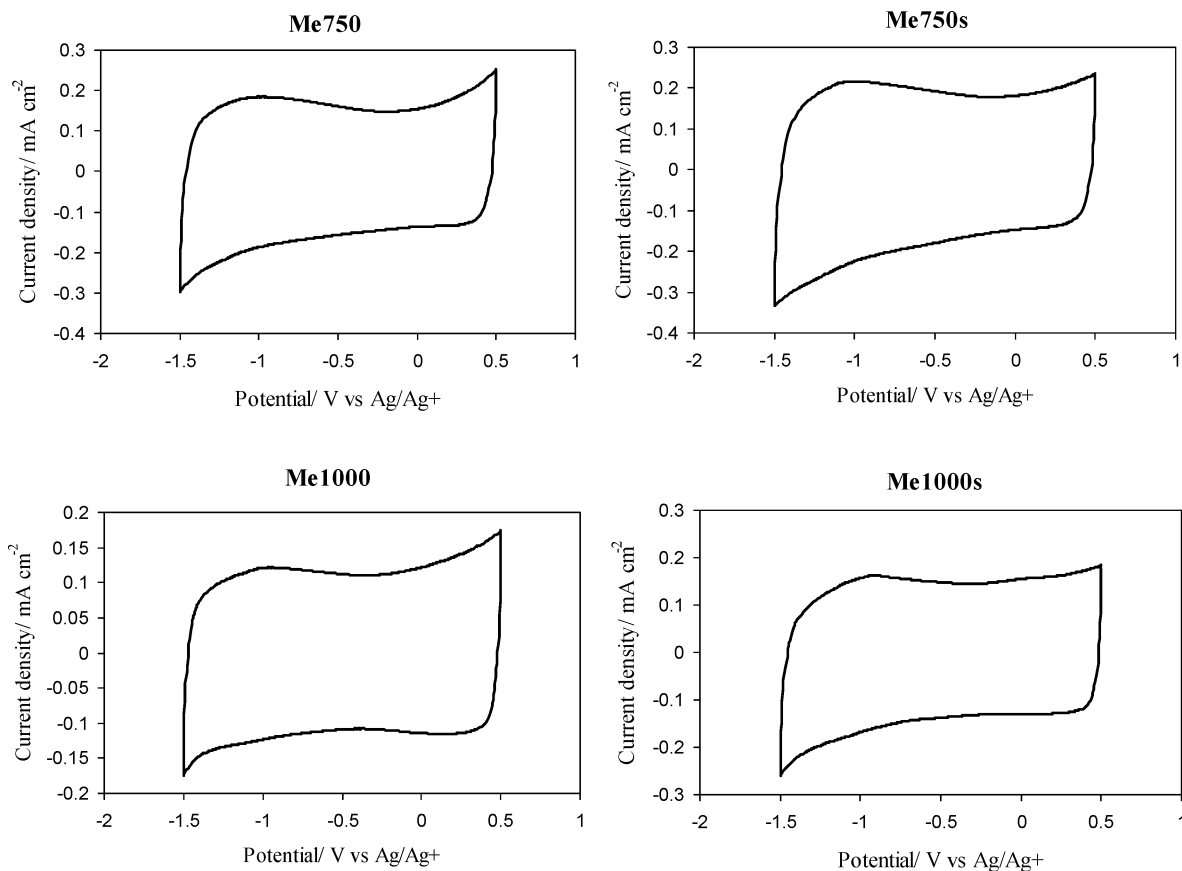


**Figure 6.** Cyclic voltammograms of samples heat-treated at 750 and 1000 °C in 1 M TEABF<sub>4</sub>/PC, potential range  $-1.5$  to  $0.5$  V vs Ag/Ag<sup>+</sup>, sweep rate =  $1$  mV/s, three-electrode cell. The thickness and mass of the electrode were ca.  $100$   $\mu$ m and  $8$  mg, respectively.

trolytes. For instance, the value for Me750 was  $37.49$  F/g, which corresponds to  $0.08$  F/m<sup>2</sup>. Interestingly, however, less-porous samples carbonized at higher temperatures showed good capacitive behavior, i.e.,  $20.61$  F/g ( $1.21$  F/m<sup>2</sup>) for Me1000s. Considering the poor surface area of this sample ( $17$  m<sup>2</sup>/g), it is clear that the contribution of the double-layer capacitance to the overall capacitance is negligible. Therefore, the faradaic interactions, although much less significant than those in H<sub>2</sub>SO<sub>4</sub> and KOH, were suggested.

From the obtained results, we can conclude that the nitrogen-enriched carbons prepared from melamine resins showed good capacitive behavior in KOH despite the absence of protons that were initially thought to be responsible for the high capacitance in an acidic electrolyte. Even in a

nonaqueous medium, some interesting results were obtained. All these data put a new insight into the capacitive behavior of poorly porous carbon with a significantly high content of nitrogen atoms. We believe it will be possible to clarify the exact mechanism of pseudocapacitive interactions between the ions and nitrogen atoms through the selective modification of the carbon electrode surface and subsequent careful evaluation of their capacitive behavior in various electrolytes. Work on this issue is being conducted.

**Acknowledgment.** D.H. is grateful to the Japan Society for Promotion of Science (JSPS) for the financial support.

CM060146I